

THE PRINCIPLES OF TWO STAGE BETATRON AND MOMENTUM COLLIMATION IN CIRCULAR ACCELERATORS

THOMAS TRENKLER and JEAN BERNARD JEANNERET

CERN, Geneva, Switzerland

(Received 9 July 1993; in final form 23 January 1995)

In future super-conducting hadron colliders a big flux of particles shall drift towards the vacuum chamber which must be trapped in dedicated warm beam cleaning sections to prevent the magnets from quenching. Here we describe the optical and kinetic principles which must be followed to set up an efficient two-stage collimation system, which is able to perform this kind of beam cleaning. Particles may be lost betatronically and due to momentum deviations. These two aspects demand different requirements from the collimation system. We show that a system fulfilling both tasks seems feasible.

KEY WORDS: Collimation, beam cleaning, collider

1 INTRODUCTION

Traditional collimation systems in particle accelerators shall protect experiments from background radiation or particles. New super-conducting proton colliders like the Large Hardron Collider (LHC) demand in addition sophisticated beam cleaning systems to prevent quenches in the magnets induced by particle losses. Detailed studies show that non-negligible particle losses occur transversely¹ as well as longitudinally.^{2,3} This implies the need of betatron collimation in the transverse phase space and of momentum or more correctly combined momentum and betatron collimation for off-momentum particles⁴. Particles hitting a collimator jaw interact in many different ways with the collimator material as for instance described by Van Ginneken⁴ or by Jeanneret and Trenkler.⁵ Inelastic interactions (a phenomenon often quite improperly called ‘absorption’) in the jaws produce secondary particles which may have low fractional energies (in the case of LHC energies $\approx 1/10$ times the initial energy) which will be swept out by the warm magnets of the cleaning insertion and can thus be considered as trapped by the system. Their particular fate is out of the scope of this paper and is studied with appropriate tracking codes.⁶ A more severe fact is that particles may fall on the collimator with very small impact parameters

⁴Pure betatron collimation can be made in dispersion free sections, while pure momentum collimation would request vanishing beta functions, a condition which cannot be satisfied.

(Some measurements have been done in the SPS antiproton-proton collider⁷ and a detailed study of impact parameter distributions has for instance been investigated by Risselada⁸ or by Seidel.⁹). These particles may be scattered out of a jaw nearly elastically and with increased amplitude. These particles are very likely to be lost in an aperture restriction in the machine before returning to the collimation section. Secondary collimators placed behind primary ones in an appropriate way can be used to trap the major fraction of these so called elastically scattered secondary particles. The aperture of these secondary collimators must of course be such that they never interfere with particles which have not touched a primary jaw before. The particles scattered by the primary jaws escaping even the secondary collimators form a beam halo, which we will call secondary beam halo. This halo plays a crucial role in what follows. We restrict ourselves to single-pass two-stage collimation systems in the sense that secondary collimators absorb all particles falling on them and that we do not analyze the possibility that secondary particles might repeatedly pass the collimation system. We consider these mechanisms somehow as higher order perturbative effects. Here we set up rules to minimize the extreme amplitudes of the secondary beam halo. These are defined by geometrical (optical) properties of the system rather than by the true scattering mechanisms in the jaws. Once the set up of the system is optimized in this sense, one has to apply simulation codes¹⁰ considering all the effects neglected so far, i.e. multi-turn, true scattering, transparency of secondary jaws, misalignment etc.

2 THE NEED OF TWO-STAGE COLLIMATION SYSTEMS

While in this paper we concentrate our attention on optical considerations, we nevertheless briefly explain why beam cleaning is an important problem in multi-TeV proton colliders and why a two-stage collimation system is necessary. We already mentioned the sensitivity of super-conducting magnets to beam losses. The need of high luminosities, obtained with high beam intensities¹¹ for the LHC machine, is making the problem even more serious.

A third kind of consideration is related to the scattering of protons in matter. If a proton is not 'absorbed' in a primary collimator jaw, it will interact elastically by doing multiple Coulomb scattering (always) and sometimes nuclear elastic scattering. The average angle of scattering of these two processes approximately scales like $1/p$, p being the beam momentum. Typical angles of scattering are given in Table 1 for a jaw made of one nuclear interaction length of aluminum. This angle must be compared to the r.m.s beam divergence $\sigma' = \sigma/\beta$, where σ is the r.m.s. beam radius and β the betatron function. The divergence σ' scales like $1/\sqrt{p}$. The numbers in Table 1 are computed with a β value of 100 meters and a normalised emittance $\varepsilon_n = \gamma\sigma^2/\beta = 3.75\mu\text{m}$, where γ is the Lorentz factor.

The fact emerging from Table 1 is that at low energy ($p < 100$ GeV/c), the scattering angles θ_{scat} are very large and therefore most of the scattered protons leave the acceptance of the machine near the collimator jaw. As well, their density in the transverse phase-space is strongly diluted. In the TeV range in contrast, the scattering angles are between the r.m.s beam divergence σ' and the acceptance of the machine. The protons which escape the primary collimators are almost all candidates for touching the vacuum chamber far downstream of the primary jaw, therefore justifying a robust set of secondary collimators acting as much as possible as absorbers. As a curiosity, we see that at asymptotic energies

TABLE 1: Comparison of r.m.s. beam divergence with typical scattering angles in one nuclear interaction length of aluminium.

$p(\text{TeV}/c)$	$\sigma'(\mu\text{rad})$	$\theta_{\text{scat}}(\mu\text{rad})$
0.03	35	1500
0.5	8.5	90
5	2.7	9
50	0.85	0.9
500	0.27	0.09

($p > 100 \text{ TeV}/c$), the beam cleaning might become easier again. When $\theta_{\text{scat}} \ll \sigma'$, the protons would stay well inside the acceptance after scattering, until they are finally absorbed after many turns and several traversals of the primary jaws. This effect is already present in the few TeV range, but is not dominant.

3 NUMERICAL EXAMPLE

To illustrate numerically some results and to help comparing different systems with each other, we will use some identical basic parameters in further sections. The jaws of the primary collimators will always be retracted by $n_1 = 6$ normalised transverse r.m.s. beam radius and the jaws of the secondary collimators always by $n_2 = 7$. All other quantities will be deduced from these two numbers. These numbers are presently a kind of canonical set used for LHC collimation studies. They can of course be changed to any other value for another application.

4 ONE-DIMENSIONAL BETATRON COLLIMATION

This subject has been discussed in a simple way by Teng¹² already in 1969. A modern approach to this topic has first been considered by Jeanneret¹³ and has found a final form by Burnod and Jeanneret¹ and Maslov *et al.*¹⁴ soon afterwards. A system built according to these principles is working in the proton ring of the HERA machine.⁹ Here we present the final results.

We assume that the optics of the collimation section is linear and uncoupled which can to a good approximation be achieved in reality. Throughout the paper we use normalised coordinates (capital letters), i.e.

$$\begin{pmatrix} Y \\ Y' \end{pmatrix} = \frac{1}{\sigma_y} \begin{pmatrix} 1 & 0 \\ \alpha_y & \beta_y \end{pmatrix} \begin{pmatrix} y \\ y' \end{pmatrix} \quad (1)$$

where y and y' are the real coordinate and the real divergence in either of the transverse planes (x : horizontal and z : vertical plane). Thus we measure coordinates in units of σ and

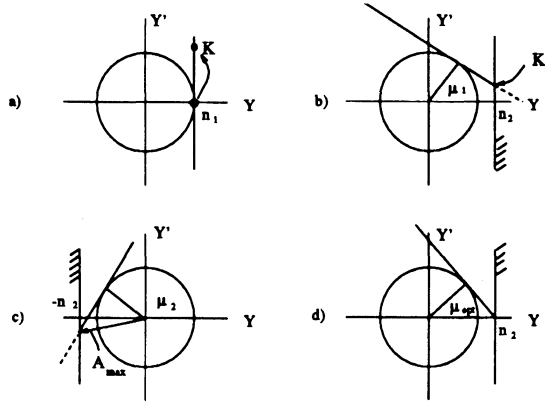


FIGURE 1: (a) Particles hitting primary collimator, (b) and (c) secondary particles intercepted by secondary collimators, (d) optimum phase advance for secondary collimators.

divergences in units of σ' where σ and σ' are transverse beam size and divergence. Linear transfer matrices reduce to rotation matrices in these coordinates

$$M = \begin{pmatrix} \cos \mu & \sin \mu \\ -\sin \mu & \cos \mu \end{pmatrix} \quad (2)$$

where μ is the phase advance in the plane considered. The Courant-Snyder invariant (action) reads $\varepsilon_y = Y^2 + Y'^2$ in these coordinates and we define its square root $A_Y = \sqrt{Y^2 + Y'^2}$ as amplitude in the corresponding plane.

With the assumptions made here we can study one-dimensional collimation systems in either of the transverse planes for the moment. If collimators are not set at too big apertures particles drift slowly towards them. Hence the time scale for filling (nearly) each point of its transverse phase ellipse at the longitudinal location of the collimator due to irrational tunes is much shorter than the time scale for drifting transversely. As a consequence particles will touch a primary collimator at their outermost spatial excursion in phase space with only very small impact parameter which is negligible compared to the dimensions of the beam^b, i.e. its coordinates are $Y = n_1$, $Y' = 0$, or non-normalised $y = n_1\sigma$ and $y' = -(\alpha/\beta)y$.

Figure 1(a) shows a particle touching a primary jaw which is supposed to be set at an aperture of $n_1\sigma$ from the beam axes. Assume that the particle receives an elastic kick of magnitude K in the primary jaw as is indicated in Figure 1(a). Other particles will get kicks of different magnitude and sign and thus fill the vertical line at the distance $Y = n_1$ from the origin directly after leaving the primary jaw.

^bThe impact parameter plays of course an important role for the scattering dynamics in the jaw and has thus a considerable influence on the efficiency of the collimation system. Here we are not interested in these effects as we discuss only geometrical aspects.

The action of a secondary jaw of aperture^c $n_2 \sigma$ and at a phase advance μ_1 (and $\mu_2 > \pi$) downstream of the primary jaw on these particles is described in Figure 1(b) and (c). The transfer matrix rotates the vertical line by the corresponding phase advances and all particles with excursions $Y_2 > |n_2|$ at phase advances μ_1 and all with excursions $Y_2 < -|n_2|$ at μ_2 are intercepted by the secondary jaws (dashed line). Two secondary collimators are necessary to cut particles from both sides of the line.

The critical kick K_c a particle must receive at least in the primary jaw to be intercepted by the secondary one can easily be extracted from these figures or by simple calculations using the transfer matrix ($Y_2 = n_2 = n_1 \cos \mu + K \sin \mu$)

$$K_c = \frac{n_2 - n_1 \cos \mu}{\sin \mu}. \quad (3)$$

To catch as many as possible of the secondary particles, or in other words, to catch the smallest possible amplitudes $A = \sqrt{n_1^2 + K^2}$ one has to place the secondary jaws such that the absolute value of K_c gets a minimum. This case is shown in Figure (d) and can as well be obtained by looking for the extreme values of K_c as a function of μ in (3):

$$\cos \mu_{\text{opt}} = n_1/n_2, \quad (4)$$

i.e. once n_1 and n_2 have been chosen, μ_{opt} is deduced. We get

$$K_{c,\text{opt}} = \sqrt{n_2^2 - n_1^2} \quad (5)$$

and a maximum amplitude in phase space of particles escaping the secondary jaw of

$$A_{\text{max,opt}} = \sqrt{n_1^2 + K_{c,\text{opt}}^2} = n_2. \quad (6)$$

We will call these particles the particles of the secondary beam halo in the sequel. The limit $A_{\text{max,min}} = A_{\text{max,opt}}$ is an absolute one. A collimator located at distance n_2 from the beam axis cannot cut on amplitudes smaller than n_2 . With our numerical set of Section 3, $\mu_{\text{opt}} \approx 30^\circ$ and $A_{\text{max,opt}} = 7$.

Summarizing we can state that the phase advance between primary and secondary collimators is the critical quantity defining the maximum excursions of the secondary beam halo^d. One secondary collimator should be set at a phase advance μ_{opt} downstream of the primary collimator and one at its complement $\pi - \mu_{\text{opt}}$ on the opposite side of the beam.

^cThe aperture n_2 must be bigger than n_1 to avoid that particles touch a secondary jaw before they touch the primary one. Its explicit value must be fixed from misalignment considerations.

^dThis is not the only quantity defining the efficiency of the collimation system, as impact parameters and thus β -functions at the primary jaw¹ and betatron-tunes^{8,9} play an important role. Also tertiary particles are emitted by secondary collimators.

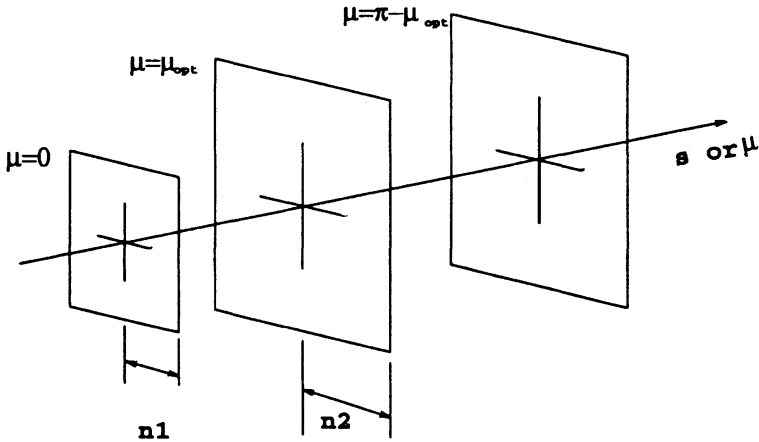


FIGURE 2: A two-dimensional collimation system with horizontal and vertical jaw. The optics is chosen with the property of equal phase advance in the two planes.

5 TWO-DIMENSIONAL BETATRON COLLIMATION WITH UP-RIGHT COLLIMATOR JAWS

A two-dimensional (X, Z) collimation system cannot be reduced to two uncoupled one-dimensional systems. The basic reason is related to the scattering of the particles in the primary jaws which is isotropic azimuthally in the $X'-Z'$ plane (apart from distorting multiple coulomb scattering edge effects) around the line of flight before scattering. This implies for example that a particle oscillating in the X -plane can be scattered into the Z -direction ('orthogonal scattering'). This effect has already been discussed by Bryant and Klein¹⁵ and by Jeanneret.¹⁶ We will approach this four-dimensional problem by a simple case, where collimator jaws are either horizontal or vertical. In addition, we confine ourselves to the special case of a symmetric low- β optics for the collimation system. A low- β optics has no special property here, except that it has equal phase advances in both planes, which simplifies our considerations and allows for comparison with the system discussed in Section 6. Collimation in other optics is discussed in Section 7.

5.1 Collimators at $\mu = \mu_{opt}$ and $\pi - \mu_{opt}$

We first install collimators the same way it was done in Section 4, extended to two dimensions. There will be a primary jaw at a distance n_1 from the beam axis in both the X and the Z planes and four secondary jaws at the phase advance $\mu = \mu_{opt}$ at a transverse distance $\pm n_2$, two in each plane. Similarly four jaws are installed at $\mu = \pi - \mu_{opt}$, as shown schematically in Figure 2. The equal phase advance in both planes makes the system completely

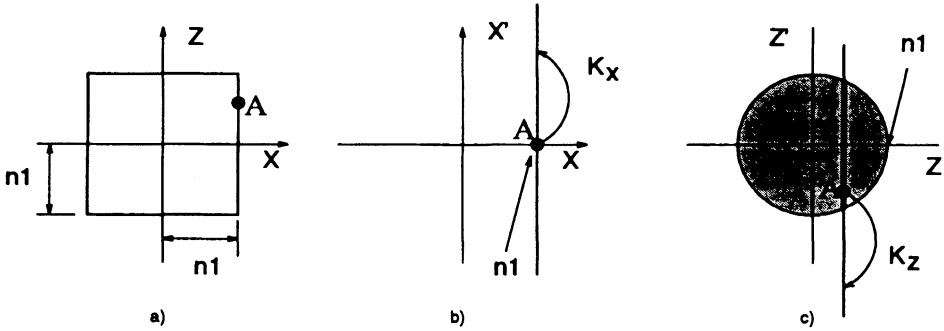


FIGURE 3: A particle touches the X-jaw in A and is scattered (a). In the X phase-space, the scattered particles lie all along a line, because of the fixed value of X (b). In contrast, every $|Z| < n_1$ value is possible, allowing for each Z all the amplitudes $|Z| < A_Z < n_1$, then K_Z adds to Z' (c).

X-Z symmetric. We can therefore consider the case of particles which touch the X-jaw. An exchange of the X and Z coordinates will give the results for particles scattered on the vertical jaw.

We consider again a proton which diffuses slowly and which has a betatron amplitude $A_X \cong n_1$, while $A_Z < n_1$, ensuring that after some diffusion the X-jaw is touched. Then to a very good approximation we have before scattering $X_1 = A_X = n_1$ and $X'_1 = 0$, while $|Z_1| < n_1$. The limit of the Z coordinate is set by the presence of the vertical primary jaw, as for $A_Z \geq n_1$, the particle would be intercepted by the vertical collimator. The elastic scattering process adds angular kicks K_X and K_Z of arbitrary value to the particle. The coordinates of the particle become

$$X_1 = n_1 \quad (\text{unchanged}) \quad X'_1 = K_X \quad (7)$$

$$Z_1 < n_1 \quad (\text{unchanged}) \quad Z'_1 = K_Z + Z'_0 \quad (8)$$

This is illustrated in Figure 3. We note that Z'_1 is the addition of a scattering angle and of a betatron one because the particle is not necessarily at its maximum amplitude in the Z plane. We are interested to find the boundaries of the amplitude of the secondary halo. We must therefore consider arbitrary values for K_X and K_Z , such that the addition of the betatron angle Z'_0 is changing nothing in practice for our study. But formally it is there and whenever true scattering is considered, it must be present. We now transport the particles to $\mu = \mu_{opt}$

$$X_2 = X_1 \cos \mu_{opt} + X'_1 \sin \mu_{opt} = n_1 \cos \mu_{opt} + K_X \sin \mu_{opt} \quad (9)$$

$$Z_2 = Z_1 \cos \mu_{opt} + Z'_1 \sin \mu_{opt} = Z_1 \cos \mu_{opt} + Z'_1 \sin \mu_{opt} \quad (10)$$

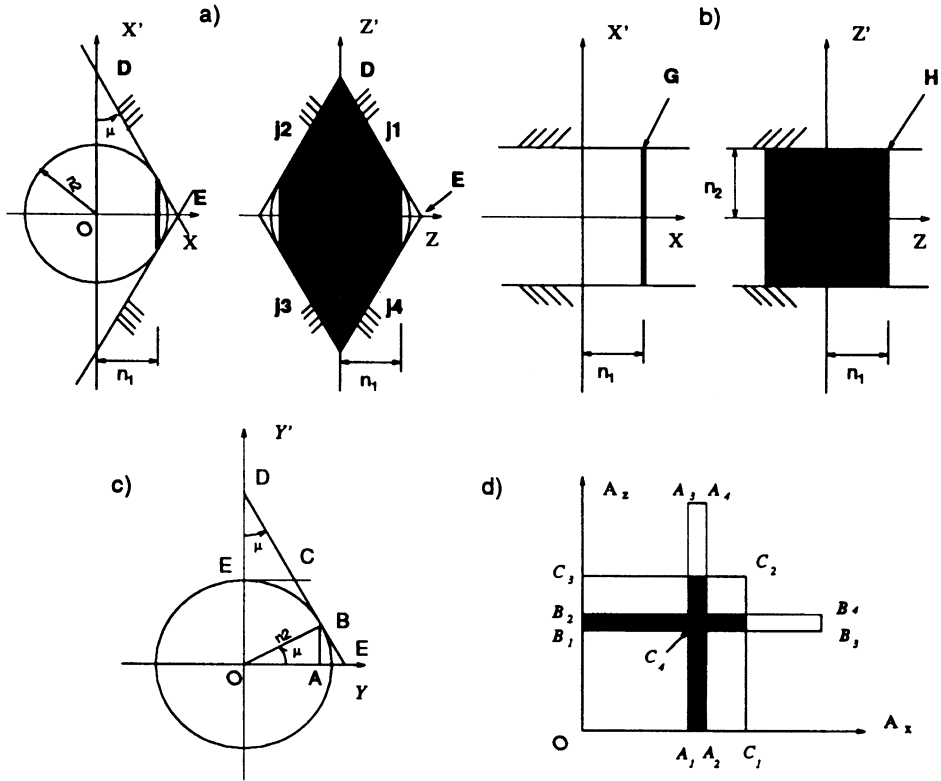


FIGURE 4: The distribution of the secondary halo in the phase-space. (a) with secondary collimators at μ_{opt} and $\pi - \mu_{opt}$. The Z -plot shows that two jaws are needed at μ_{opt} , at $Z = +n_2$ (j1) and $Z = -n_2$ (j3). Similarly, j2 and j4 are needed at $\pi - \mu_{opt}$. (b) with a secondary collimator (4 jaws) at $\mu = 90^\circ$. The maximum allowed amplitudes are equal in both planes (point G and H). (c) A figure which allows to get all the quantities needed to compute the maximum amplitudes. It is enough to fix n_1, n_2 and $\cos \mu = \cos \mu_{opt} = n_1/n_2$. Then $OD = n_2 / \sin \mu_{opt} = n_2^2 / (n_2^2 - n_1^2)^{1/2}$. With the combined system ($\mu_{opt}, 90^\circ$ and $\pi - \mu_{opt}$), the secondary halo is restricted to the segment AB in $X - X'$, while in $Z - Z'$ it occupies the surface $OABCEO$ (not shaded to keep some clarity). (d) An amplitude plot for the secondary halo of the three cases. The system (a) populates the rectangle A ($A_1 A_2 A_3 A_4$). Exchanging X and Z populates the rectangle B . The system (b) populates the area $A_1 C_1 C_2 C_3 B_1 C_4 A_1$. The combined system (c) occupies the shaded area which is the intersection of what is allowed to (a) and (b). $OA_1 = n_1, OA_2 = n_2, OC_1 = (n_1^2 + n_2^2)^{1/2}, B_1 B_3 = A_1 A_3 = OD$.

The particle passes the collimator at μ_{opt} if $X_2 < n_2$ and $Z_2 < n_2$ which using (9) and (10) solved for K_X and Z' becomes

$$K_X < K_{X,c} = \frac{n_2 - n_1 \cos \mu_{opt}}{\sin \mu_{opt}} \tag{11}$$

and

$$Z'_1 < Z'_c = \frac{n_2 - Z_1 \cos \mu_{opt}}{\sin \mu_{opt}} = \frac{n_2}{\sin \mu_{opt}} - Z_1 \cot \mu_{opt} \tag{12}$$

Without surprise, condition (11) is identical to (3) obtained in the one-dimensional case. But, even if the Z-condition is similar in its structure to the X-condition, the fixed value n_1 in (11) is replaced by the variable Z_1 in (12) which can have any value inside $|Z_1| < n_1$. In the normalised vertical phase-space at the location of the primary collimator, (12) is a straight line of slope $-\cot \mu_{\text{opt}}$, which is the edge of the collimator located at μ_{opt} . This is illustrated in Figure 4(a) for both planes. The geometry of the figures for X and Z is identical. The additional lines, all of slope $\pm \cot \mu_{\text{opt}}$ represent the jaws $\pm n_2$ at both μ_{opt} and $\pi - \mu_{\text{opt}}$. Even if there is only one positive primary X-jaw, because of ‘orthogonal scattering’ and of negative Z-coordinate at $\mu = 0$, two jaws are necessary to cut the secondary halo at a given phase advance. Adding a primary Z-jaw implies four jaws at each phase advance where secondary jaws are installed.

The difference between the two planes is the range of the Z coordinate as opposed to the fixed $X = n_1$ value. In the Z phase-space, when $Z_1 = 0$, Z'_1 can reach very large amplitudes, while when $Z_1 = n_1$, the allowed excursion of Z'_1 is efficiently limited. The coordinates of some important locations are given in Figure 4c. The extreme amplitudes allowed to the secondary beam halo in each plane are obtained by searching for the largest distance to the origin in the shaded areas in Figure 4a. The maximum amplitude in the X-plane is given by the distance $A_{X,\text{max}} = OB = n_2$, while in the Z-plane $A_{Z,\text{max}} = OD = n_2^2 / \sqrt{n_2^2 - n_1^2}$. We also deduce that $A_{X,\text{min}} = OA = n_1$ and $A_{Z,\text{min}} = 0$. We can now build a boundary plot in the $A_X - A_Z$ plane. The extreme values of A_X and A_Z are not correlated to each other. Therefore the secondary halo produced at the horizontal primary jaw populates the upright rectangle A of Figure 4(d). Of course the density inside the rectangle will not be uniform. Simulations show that high amplitudes are scarcely populated.¹⁰ Even for homogeneous scattering the triangular cut in $Z - Z'$ near point D of Figure 4(a) depopulates the largest amplitudes. But nevertheless, if a collimation system has to be very efficient, these large amplitudes are sufficiently present to be considered. Using our numerical set (Section 3), we get $A_{X,\text{max}} = 7$, $A_{Z,\text{max}} = 13.6$ (and vice-versa for the protons scattered by the Z-primary jaw, which populates the rectangle B in Figure 4(d)) and $A_{\text{max}} = \sqrt{A_{X,\text{max}}^2 + A_{Z,\text{max}}^2} = 15.3$.

We observe the important fact that what is optimum in a one-dimensional system is not optimum at all in a two-dimensional one. The figure of merit of a system, which might be the ratio $r = A_{\text{max}}/n_1$, is for our 2-dim system $r = 2.55$ while $r = 7/6 = 1.17$ in a 1-dim system (see Section 4).

5.2 Collimators at $\mu = 90^\circ$

A way to improve the system is to add four jaws at $\mu = 90^\circ$, also at a transverse distance $X = Z = n_2$.

Let us first discuss a system with only these jaws at $\mu = 90^\circ$. Replacing $\mu = \mu_{\text{opt}}$ by $\mu = 90^\circ$ in (11, 12), we get the maximum kicks allowed to pass the secondary jaws

$$K_X = X_2 < n_2 \quad Z'_1 = Z_2 < n_2 \quad (13)$$

The lower limit for both K_X and Z'_1 is zero. The dependence of X_2 and Z_2 on X_1 and Z_1 disappears. In the phase-space (Figure 4b) the jaws at 90° appear as horizontal boundaries

of equation $X' = n_2$ and $Z' = n_2$. They limit the maximum amplitudes to (using conditions (13))

$$A_{X,\max} < \sqrt{X_{1,\max}^2 + K_{X,\max}^2} = \sqrt{n_1^2 + n_2^2} \quad (14)$$

$$A_{Z,\max} < \sqrt{Z_{1,\max}^2 + Z'_{1,\max}} = \sqrt{n_1^2 + n_2^2} \quad (15)$$

The lower limits are $A_{X,\min} = n_1$ and $A_Z = 0$ in the case of scattering on the primary X-jaw.

The secondary beam halo of a collimation system with secondary jaws only at 90° would occupy in the amplitude plot the surface C (drawn in Figure 4(d)). The maximum amplitude is given by the diagonal of the occupied surface, $A_{\max,90^\circ} = \sqrt{2(n_1^2 + n_2^2)}$. With our numerical set, we get $A_{\max,90^\circ} = 13.04$ and a figure of merit $r=2.17$. This system is also not a good one by itself.

5.3 Collimators at $\mu_{\text{opt},90^\circ}$ and $\pi - \mu_{\text{opt}}$

If we now look at Figure 4(d), we see that by combining the three phase advances $\mu_{\text{opt},90^\circ}$ and $\pi - \mu_{\text{opt}}$, the resulting surface allowed to the secondary halo is much smaller (see Figure 4(d)). It is obtained simply by the intersection of the two rectangles A and B with the surface C . The maximum amplitudes are $A_{X,\max} = n_2$ and $A_{Z,\max} = n_2 / \cos(\frac{\pi}{4} - \frac{\mu_{\text{opt}}}{2})$, deduced by geometry from Figure 4c. With our numerical set, $A_{X,\max} = 7$, $A_{Z,\max} = 8.04$ and $A_{\max} = 10.66$, yielding $r = 1.78$.

We now get better results, but we are far from the performance offered by the one-dimensional theory, which in practice does not apply to most of the existing colliders. For instance in machines like the LHC the primary collimators should be set in the vicinity of the short term dynamical aperture. In LHC this dynamical aperture is approximately circular in amplitude space, which is not at all accounted for by the system described in this section, as the radial amplitude of the primary beam goes up to $\sqrt{2}n_1$ at the 45° -symmetrinal in Figure 4 (Jeanneret¹⁶).

We will see in the next section what ultimate performance can be reached with a two-dimensional collimation system in the optics of this section. We will demonstrate also that the choice of the three phases made empirically here is a quite good one.

6 TWO-DIMENSIONAL BETATRON COLLIMATION WITH COLLIMATORS OF CIRCULAR APERTURE IN SYMMETRIC LOW-BETA INSERTIONS

According to the final remarks of the preceding section it seems natural to consider collimators with circular aperture in normalised transverse space, i.e. with generally elliptical aperture at locations of different horizontal and vertical β . Machines like the LHC have to operate at different energies. This implies that the radius of the circular collimator should scale like $1/\sqrt{E}$ which is of course mechanically impossible. A good way (chosen by the authors for an LHC collimation system) is to approximate the circles (ellipses) by a

regular octagon of straight jaws in normalised coordinates i.e. an octagon with dimensions scaled with $\sqrt{\beta}$ in each transverse direction in real physical space. Strictly speaking these jaws cannot be located at exactly the same longitudinal coordinate but must be placed one after the other with the possible exception of parallel jaws. For the following considerations all these approximations are irrelevant and we use here systems of collimators of vanishing length and circular aperture in normalised transverse space as shown in Figure 5(a). In this section we confine ourselves to the special optics of the previous section namely a low- β section with equal β -functions and thus (for us more important) equal phase advances in both transverse planes. We do that for two reasons:

- One can describe the collimation system analytically.¹⁷
- This kind of optics has for a long time been considered to be adequate for the LHC cleaning system.¹⁸

As in Section 4 we can argue that particles are at their outermost excursions in both transverse planes when touching a primary collimator: The envelope of the transverse motion at the location of the primary collimator is a rectangle parallel to the axes in the X-Z plane. Due to the incommensurability of the tunes there is a certain chance to find the particles close to the corners of this rectangle. As the transverse drift mechanisms pushing the particles to the collimator have a long time scale compared to the time a particle needs to return to one of the corners it is evident that the particle will hit the collimator when being in one of these extreme states of its motion. Of course impact parameters might be a bit bigger than in the one-dimensional case as it takes more time to find the particle at its extreme excursion in both planes than only in one plane. Nevertheless they will still be small such that we can neglect them in the following calculations.

The touching particle indicated in Figure 5(a) has thus the following coordinates:

$$X = n_1 \cos \alpha, \quad X' = 0, \quad Z = n_1 \sin \alpha, \quad Z' = 0 \quad (16)$$

Again we are interested in the fate of particles receiving elastic kicks in the collimator. As in the previous section the kick can now point into any direction in transverse space as indicated in Figure 5(a). Thus immediately after leaving the collimator the coordinates of the particle will eventually transform into

$$X = n_1 \cos \alpha, \quad X' = K_X, \quad Z = n_1 \sin \alpha, \quad Z' = K_Z, \quad (17)$$

where K_X and K_Z are the normalised kicks in either direction. The action of a secondary collimator on these particles may be studied by asking for the kick a particle must obtain for falling on the aperture of this collimator. We again assume a circular secondary collimator with aperture $n_2\sigma$ and at a phase advance μ from the primary collimator. The particle of (17) is transported in each plane by the transfer matrix (2) to the location of the secondary collimator, i.e. the coordinates of the particle at the location of the secondary collimator are

$$\begin{pmatrix} X_{\text{sec}} \\ Z_{\text{sec}} \end{pmatrix} = \cos \mu \begin{pmatrix} n_1 \cos \alpha \\ n_1 \sin \alpha \end{pmatrix} + \sin \mu \begin{pmatrix} K_X \\ K_Z \end{pmatrix} \quad (18)$$

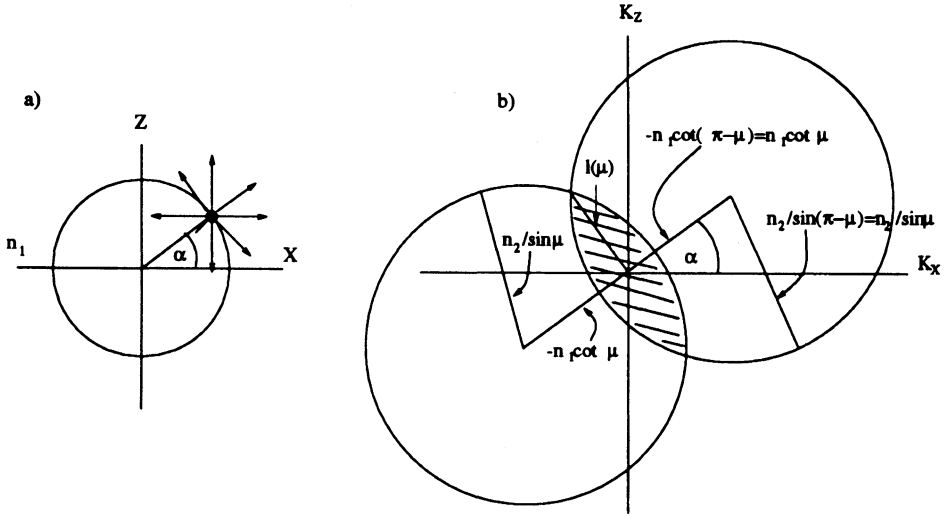


FIGURE 5: (a) Particle hitting the primary collimator at position α , (b) \vec{K} -plane of secondary particles produced at α , shaded area: Secondary beam halo particles which pass the system of two circular secondary collimators at phase advances μ and $\pi - \mu$.

or solved for the kicks

$$\begin{pmatrix} K_X \\ K_Z \end{pmatrix} = \frac{1}{\sin \mu} \begin{pmatrix} X_{\text{sec}} \\ Z_{\text{sec}} \end{pmatrix} - \cot \mu \begin{pmatrix} n_1 \cos \alpha \\ n_1 \sin \alpha \end{pmatrix}. \quad (19)$$

We ask for the kicks pushing the particles onto the aperture of the secondary collimator, i.e. on a circle of radius n_2 : $n_2^2 = X_{\text{sec}}^2 + Z_{\text{sec}}^2$. According to (19) the location of all the kicks we are asking for form thus a circle of radius $n_2/\sin \mu$ centered at the point of incidence on the primary collimator scaled by a factor $-\cot \mu$ in the plane of the kicks. This circle is the one on the upper right side of Figure 5(b). All particles with kicks outside this circle are intercepted by the collimator while those in its interior pass the collimator undisturbed. The second circle in Figure 5(b) is the corresponding one for a collimator located at a phase advance $\pi - \mu$. Only those particles lying inside the intersection of both circles (shaded area) can pass a system with the two secondary collimators considered. They form the secondary beam halo passing the whole collimation system. We want to stress that Figure 5(b) is the image in the K -plane of the secondary beam halo produced at the single point of incidence at azimuth α on the primary collimator indicated in Figure 5(a). For other points of incidence the angle α in the figure is changing but the shaded area keeps its shape, i.e. the figure is just rotated by an adequate angle.

Hence it is sufficient to study the effects of further collimators on the beam halo produced only at one point of incidence as all other configurations in the K -plane can be obtained by rotation. For simplicity we choose $\alpha = 0$ (see Figure 6).

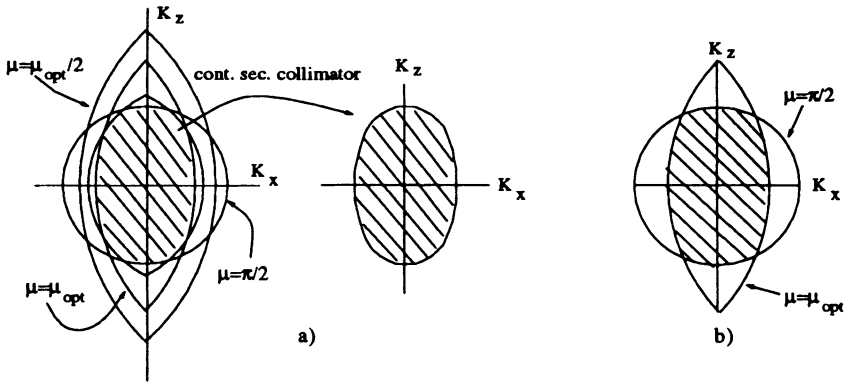


FIGURE 6: (a) The continuous secondary collimator and (b) its approximation by the 90° , μ_{opt} and $\pi - \mu_{opt}$ collimation system. K -plots for particles incident at $\alpha=0$ on the primary jaw.

6.1 Impact on the primary jaw at $\alpha = 0$

The best collimation system of the type considered here is one with secondary collimators at all possible phase advances between 0° and 180° , i.e. a continuous secondary collimator between these phase advances^e. Figure 6(a) shows the K -plane of the secondary beam halo of such a system. We are able to give an analytical formula for its boundary curve which is the envelope of all the circles corresponding to collimators at different phase advances μ . These circles can be parameterized by

$$\begin{pmatrix} K_X \\ K_Z \end{pmatrix} (\mu, \beta) = \frac{n_2}{\sin \mu} \begin{pmatrix} \cos \beta \\ \sin \beta \end{pmatrix} - n_1 \cot \mu \begin{pmatrix} 1 \\ 0 \end{pmatrix} \tag{20}$$

where μ is the phase advance and β the running parameter on the circle. The condition defining the envelope is that it should be tangent to one of the curves in each of its points or expressed in formulae

$$\partial_\mu \vec{K} \parallel \partial_\beta \vec{K} \iff \partial_\mu K_X \partial_\beta K_Z - \partial_\beta K_X \partial_\mu K_Z = 0. \tag{21}$$

Extracting β as a function of μ from this equation and inserting it into (20) finally yields the envelope parameterized by the phase advance μ of the corresponding circle touching at this point of the envelope

^eThis is of course only a very theoretical model. Not only hardware problems occur but also the fact that particles have vanishing impact parameter in this system causes larger outscattering of the particles than for discrete secondary collimators. Here we consider that the secondary collimator absorbs all particles falling on it. Nevertheless the system is of great interest as it is the theoretical limit of a two-stage collimation system in a X - Z symmetric optics.

$$K_{\text{env},X}(\mu) = \frac{n_2^2 - n_1^2}{n_1} \cot \mu \quad (22)$$

$$K_{\text{env},Z}(\mu) = \frac{n_2 \sqrt{n_1^2 - n_2^2 \cos^2 \mu}}{n_1 \sin \mu}. \quad (23)$$

As a curiosity we can give the shaded area of Figure 6(a)

$$A = \pi n_2 \sqrt{n_2^2 - n_1^2}. \quad (24)$$

The root in equation (23) is real only if

$$\cos^2 \mu \leq n_1^2/n_2^2. \quad (25)$$

This shows that only phase advances fulfilling (25) define the envelope in the K -plane, as can also be seen from Figure 6(a). Thus the collimators with phase advances outside this range are useless for collimation. In condition (25) we find again the phase advance μ_{opt} introduced for one-dimensional collimation systems in Section 4, as it is equivalent to

$$\mu_{\text{opt}} = \arccos \frac{n_1}{n_2} \leq \mu \leq \pi - \mu_{\text{opt}} \quad (26)$$

if we restrict ourselves to phase advances smaller than 180° .

By setting $\mu = \mu_{\text{opt}}$ in (22) and (23) we get $K_{\text{env},Z} = 0$ defining the extreme value of the halo on the K_X -axis. For $K_{\text{env},X}$ we find $K_{\text{env},X}(\mu_{\text{opt}}) = \sqrt{n_2^2 - n_1^2}$, the same value found for $K_{c,\text{opt}}$ in the one-dimensional case of Section 4. Conversely setting $\mu = \pi/2$ in (22) and (23) yields $K_{\text{env},X} = 0$ and $K_{\text{env},Z} = n_2$ defining the extent of the halo on the K_Z -axis. We must recall that because of the choice $\alpha = 0$, X corresponds to ‘in plane’ scattering while Z corresponds to ‘orthogonal’ scattering. The extreme values for K are identical to those obtained in the previous section. One difference is that the envelope of the beam halo in the K -plane is a rectangle for the collimation system considered there. Another difference is the magnitude of X and Z amplitudes of particles touching the primary collimator.

Figure 6(b) shows the secondary beam halo of a collimation system with μ_{opt} , $\pi - \mu_{\text{opt}}$ and 90° collimators only. Comparing it to the theoretical system we see that we sacrifice only very little on the extent of the beam halo and that further collimators only have a very small impact on the quality of the system.

From now on we will consider this system with the μ_{opt} , $\pi - \mu_{\text{opt}}$ and the 90° secondary collimators. To get an idea of the extent of the secondary beam halo we again look at its extent in the amplitude space as we did in the previous section.

6.2 Arbitrary point of impact on the primary jaw

We first consider a system with μ_{opt} and $\pi - \mu_{\text{opt}}$ collimators only and without the 90° collimator. Instead of deriving complicated analytical formulae we prefer to give the

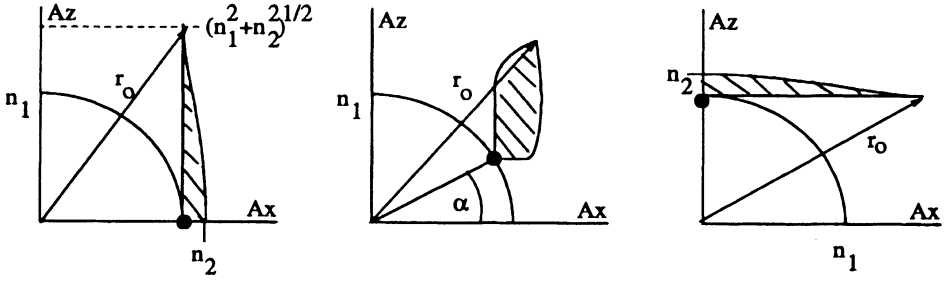


FIGURE 7: Beam halo produced at different locations on the primary collimator for the μ_{opt} and $\pi - \mu_{opt}$ collimation system. $r_0 = \sqrt{(2n_1^2 + n_2^2)}$.

corresponding figures and some quantities which can easily be calculated. Figure 7 shows the amplitude plot of the beam halos produced at different locations of impact on the primary jaws. These plots are produced by taking

$$A_X = \sqrt{X^2 + K_X^2} \quad \text{and} \quad A_Z = \sqrt{Z^2 + K_Z^2} \quad (27)$$

with X, Z given in (17) and K_X, K_Z taken from the shaded area of Figure 5(b) for $\mu = \mu_{opt}$. The outermost radial extent r_0 can easily be obtained:

$$\begin{aligned} r_0^2 &= \max(A_X^2 + A_Z^2) = \\ &= \max(X^2 + K_X^2 + Z^2 + K_Z^2) = \max(n_1^2 + K_X^2 + K_Z^2) = \\ &= n_1^2 + l(\mu_{opt})^2 = 2n_1^2 + n_2^2 \end{aligned} \quad (28)$$

where $l(\mu_{opt}) = \sqrt{n_1^2 + n_2^2}$ is the outermost radial extent in the K -plane (deduced from Figure 5(b) and μ_{opt} from (4)). We see that r_0 is indeed independent of α i.e. of the point of incidence on the primary collimator. The highest (biggest A_Z) particle in the left graph of Figure 7 is a particle moving originally in the horizontal plane and receiving the biggest possible kick in the vertical direction without touching a secondary collimator. This particle has received no kick in its plane of motion at all. A particle moving in the horizontal plane and receiving a kick only in this plane cannot survive an amplitude of n_2 as is shown in the same graph. This result is not astonishing as for this configuration the system can be regarded as one dimensional and was thus already described in Section 4.

Combining all beam halos for different points of incidence on the primary jaws, i.e. combining all figures 7 for different azimuth α finally visualizes the complete secondary beam halo passing the collimation system with secondary collimators at μ_{opt} and $\pi - \mu_{opt}$ (Figure 8) showing a considerable extent in direction of the diagonal $A_X = A_Z$ of the amplitude plot.

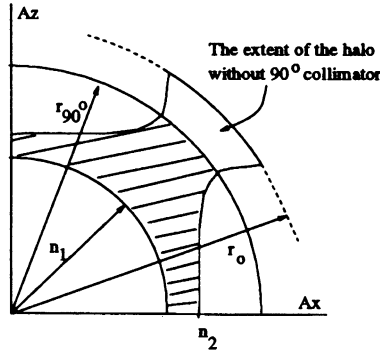


FIGURE 8: Amplitude plot of the μ_{opt} , $\pi/2$ and $\pi - \mu_{\text{opt}}$ collimation system. $r_0 = \sqrt{(2n_1^2 + n_2^2)}$, $r_{90^\circ} = \sqrt{(n_1^2 + n_2^2)}$.

Now we look at the action of the 90° collimator. The shaded area of Figure 5(b) degenerates to a circle of radius n_2 as can also be seen in Figure 6(b). Choosing

$$K_X = n_2 \cos \alpha \quad \text{and} \quad K_Z = n_2 \sin \alpha \quad (29)$$

i.e. the special kicks parallel to the point vector of incidence, we get

$$A_X = \sqrt{n_1^2 + n_2^2} |\cos \alpha| \quad \text{and} \quad A_Z = \sqrt{n_1^2 + n_2^2} |\sin \alpha|. \quad (30)$$

Thus the (quarter) circle of radius $r_{90^\circ} = \sqrt{n_1^2 + n_2^2}$ is fully populated by the secondary beam halo if the 90° collimator is alone.

Taking an arbitrary azimuth γ independent of α in equation (29) we find again $A_X^2 + A_Z^2 = n_1^2 + n_2^2$ which shows that a 90° collimator collimates 'in' and 'out of plane' particles in the same way. Further we see that the (quarter) circle of radius r_{90° actually forms the boundary of the secondary beam halo.

Thus the secondary beam halo with secondary collimators at μ_{opt} , $\pi - \mu_{\text{opt}}$ and at 90° fills the shaded area in Figure 8, being the intersection of the beam halo of the system with μ_{opt} and $\pi - \mu_{\text{opt}}$ collimators only and the system with a 90° secondary collimator. The effect of the 90° collimator can thus be characterized as constraining the radial extent of the secondary beam halo around the diagonal $A_X = A_Z$ in the amplitude plot. Or expressed in a different way, the 90° collimator is necessary for catching particles efficiently which were subject to strong orthogonal scattering in the primary jaws.^f

In this section we could show that a collimation system adapted to a dynamical aperture being circular in amplitude space is feasible.

^f Combining the four phases (i.e. 0° , 30° , 90° and 150° for our numerical set) we also define a hexagonal diaphragm in both transverse phase-spaces. Whenever strong single turn disturbances occur the secondary collimators become primary aperture limiters offering a good phase coverage.

7 BETATRON COLLIMATION IN AN ARBITRARY OPTICS

There are some arguments which make other optics preferable to the low- β insertion.

- The overall phase advance of the central drift space of a low- β insertion cannot exceed 180° . Hence the location of the 90° -collimator is very close to β^* which implies that the transverse dimensions of the beam and of the collimators get very small. This makes alignment difficult and might eventually demand different technology than the other collimators.
- Low- β insertions create high peak-values of β -functions, which in their turn have a bad influence on the dynamical aperture. This does not happen for example in a well matched FODO-structure.
- The phase-advance is the same in both planes. This makes computations easy. But different phase-advance combinations might allow to cut deeper into the secondary beam halo.
- The low- β insertion demands a dog-leg of bending magnets to sweep out secondary low energy particles. In another optics this job can at least partly be done by chromatic effects of the quadrupoles distributed in the cleaning section. This allows to filter these particles in a much more efficient way.

Unfortunately the methods developed in the previous section prove inadequate for another optics than the low- β one as the circles in the K -plane transform into ellipses not any more centered on one line and the figures change considerably from one point of impact on the primary jaw to another one. One is very soon lost in mathematical problems. Nevertheless the tools developed so far allow to judge other collimation systems. From the geometrical point of view the extent of the secondary beam halo is a measure for the quality of the system. For a given system in a given optics it is not difficult to construct numerically the envelope of the secondary beam halo in amplitude space. By changing the positions of the collimators (which we assume again to have circular aperture in normalised coordinates) one can try to minimize the horizontal, the vertical and the radial extents of the secondary beam halo. This is roughly the procedure our code COLOC¹⁰ uses for locating primary and secondary collimators in a given but otherwise arbitrary uncoupled linear optics. As β -functions need not be equal anymore the code allows to split the primary circular collimator into three groups: Jaws for horizontal collimation at large horizontal β , vertical jaws at large vertical β and jaws around the X-Z diagonal preferably at equal betas.

To get an idea about collimation in a non-symmetric optics we study regular thin lens FODO structures of different phase advances. Figure 9 shows the positions for primary and secondary collimators in one of these optics, as they have been evaluated by our code COLOC. In the following section we compare the extents of the secondary beam halos of these optics with each other and to the collimation systems discussed before.

8 NUMERICAL COMPARISON

In Table 2, we compare the different two-stage systems studied. In an accelerator which has a limited margin between the stable limit of the transverse amplitude and the short

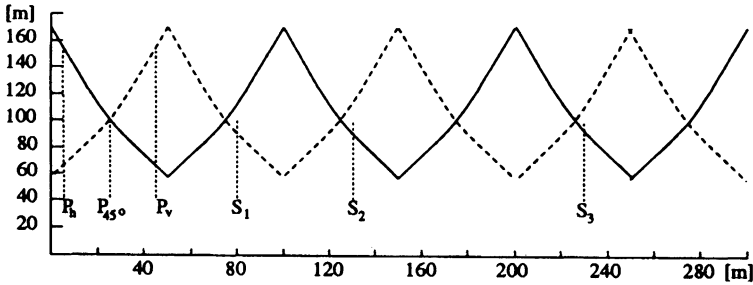


FIGURE 9: A collimation system with three secondary circular collimators and split primary ones in a thin lens FODO-structure of 60° phase advance per cell. P_h , P_v , and P_{45° : Primary collimators for the horizontal plane, vertical plane and in the symmetral of the normalised coordinate space. S_1 , S_2 and S_3 : Secondary collimators of elliptical aperture (circular in normalised coordinates).

term dynamic aperture, it is crucial that the collimation system offers the smallest possible figure of merit $r = A_{\max}/n_1$. This excludes the system made of horizontal and vertical jaws discussed in Section 5. The system of circular collimators in a low- β insertion offers a better value and has the nice property that the continuous secondary collimator can very well be replaced by the three collimators mentioned in the table. This system is however theoretically limited by the equal phase advance in both planes. Breaking this symmetry should allow to come closer to the theoretical limit of $r_{\min} = A_{\max,\min}/n_1 = n_2/n_1$ (see Section 4). This tendency can be observed in the FODO structures with continuous secondary collimator. Especially the 120° optics reaches a figure of merit close to the theoretical limit. This fact is not too surprising, as the difference of horizontal and vertical β functions take the biggest value in this optics, which causes the phase advances to propagate quite differently in both planes. Unfortunately the approximation of the continuous collimator by three discrete ones is not as perfect as in the low- β case such that realistic systems seem to be of quite equal quality in both cases. Nevertheless one shall not forget the advantages of the FODO against the low- β optics discussed in the previous section. The different phase-advances in the two planes might also be used more efficiently by breaking longitudinally the circular collimators. This subject would require a specific simulation.

9 COMBINED MOMENTUM AND BETATRON COLLIMATION

Now we turn to the collimation of off-momentum particles. To specifically collect those particles with large momentum deviation a certain value of dispersion is needed at the primary collimator. In general these particles will have some betatron emittance in addition, such that we can only talk of a combined momentum and betatron collimation. Outscattering from the primary collimator leads to the same kind of problem discussed up to now, implying the need of secondary collimators. We confine ourselves for the moment to the horizontal transverse plane as this is usually the plane where dispersion is present. Hence we have to generalize the conditions derived in Section 4 to off-momentum particles.

TABLE 2: Extent of the secondary beam halos in different collimation systems.

Optics and Sec. Collimator location Prim. Collimators at $n_1=6$ Secondary Collimators at $n_2=7$	$A_{X,\max}$	$A_{Z,\max}$	A_{\max}	A_{\max}/n_1
<u>low-β</u>				
1-dim				
$\mu_{\text{opt}}, \pi - \mu_{\text{opt}}$	7	–	–	1.17
2-dim h-v				
$\mu_{\text{opt}}, \pi - \mu_{\text{opt}}$	7	7	15.3	2.55
90°	9.2	9.2	13.0	2.17
$\mu_{\text{opt}}, 90^\circ, \pi - \mu_{\text{opt}}$	7	7	10.7	1.78
2-dim circular				
$\mu_{\text{opt}}, \pi - \mu_{\text{opt}}$	7	7	11.0	1.83
90°	9.2	9.2	9.2	1.54
$\mu_{\text{opt}}, 90^\circ, \pi - \mu_{\text{opt}}$	7	7	9.2	1.54
2-dim FODO, 3 Sec. Circular Coll. $\beta_{\max}=170\text{m}$, total length=300m				
60° per cell	7.4	7.5	9.5	1.58
90° per cell	7.4	7.5	9.6	1.60
120° per cell	7.3	7.3	9.8	1.63
2-dim, Continuous Sec. Circular Coll.				
<u>low-β</u>	7	7	9.2	1.54
FODO 60°	7.1	7.1	9.5	1.58
FODO 90°	7.1	7.1	9.2	1.53
FODO 120°	7.1	7.1	8.2	1.37

According to (1) we have to normalise dispersion as

$$\begin{pmatrix} \chi \\ \chi' \end{pmatrix} = \frac{1}{\sigma} \begin{pmatrix} 1 & 0 \\ \alpha & \beta \end{pmatrix} \begin{pmatrix} D \\ D' \end{pmatrix}. \quad (31)$$

We have omitted the index for the horizontal plane.

We do not have to consider synchrotron motion in our discussion as we are dealing with particles which are either close to the edge of the bucket or even outside. In both cases synchrotron motion gets very slow (theoretically infinitely slow) compared to transverse betatron motion.

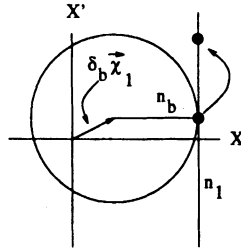


FIGURE 10: Phase space at primary collimator for momentum collimation.

9.1 Collimation Conditions for Primary Jaws

Usually particles may lose energy either by not being trapped in the bucket before acceleration or by spilling gradually out of the bucket with the effect that they will in average not be accelerated any more. Also, at sufficiently high energies even protons lose energy by synchrotron radiation. These protons, once kicked out of the bucket^{2,3} will drift towards lower momentum. Accidents (trip of a power supply, or quench of a main bending magnet, etc.) may lead to scenarios with particles of positive momentum deviation. To be able to collect particles of both signs of $\delta = \Delta p/p$ we put a primary collimator at both sides of the beam and at a distance of $n_1\sigma$ in the horizontal plane. Without loss of generality we will assume that D , δ and n_1 at the primary collimator are positive. Due to the symmetry of the configuration other combinations of signs yield the same restrictions for the absolute value of dispersion at the primary jaw.

We now derive some conditions for the normalised dispersion χ_1 at the primary collimator.

The collimator is not allowed to eat too deeply into the bucket, as particles therein may be stable even if they have a non negligible betatron amplitude. In Figure 10 we assume a particle at the edge of the bucket. The relative momentum deviation δ_b is the bucket half-width and n_b is a betatron amplitude that lies just at the dynamical aperture. The value for n_b is of course machine dependent. Hence the normalised dispersion at the primary jaw shall fulfill the condition

$$\delta_b \chi_1 + n_b = n_1 \quad \iff \quad \chi_1 = \frac{n_1 - n_b}{\delta_b}. \tag{32}$$

The maximum δ which can pass the primary collimator is defined by

$$\delta_{\max} \chi_1 = n_1, \tag{33}$$

corresponding to a particle without betatron amplitude just passing the aperture restriction.⁸

⁸It is quite improbable that particles will ever reach this value of momentum deviation. Non-linearities will blow up the betatron emittance much before such that the particles will be trapped by the collimator at much lower momentum deviation. Nevertheless this theoretical limit is of interest as a qualitative measure for the efficiency of the momentum-cut done by the collimation system. Or said in other words, it is a value for the momentum-cut which leaves some safety margin.

Inserting (32) we get

$$\delta_{\max} = \frac{n_1}{n_1 - n_b} \delta_b. \quad (34)$$

A good momentum-collimation system should do the momentum-cut as close to the edge of the bucket as possible. The value of n_b is fixed by the dynamics of the beam (dynamical aperture at the edge of the bucket) rather than by the value of n_1 . Hence by increasing n_1 , δ_{\max} approaches the bucket half-height. Formula (32) shows that the dispersion at the primary collimator has to increase with n_1 . In a real machine there will only be a limited possibility for doing so. Furthermore this can of course only be done if one investigates two independent collimation systems for momentum and betatron collimation. Otherwise n_1 is fixed by betatron collimation, and one must check whether δ_{\max} lies in an acceptable range. In¹⁸ we used this procedure to show that a combined system seems feasible for LHC. An acceptable value of δ_{\max} is also related to the ratio $A_{\text{ring}}/D_{\text{max,ring}}$. This cannot always be taken into account analytically when one considers the secondary beam halo and requires numerical simulations.

9.2 Collimation Conditions for Two-Stage Collimation

We have to study how secondary collimators collect particles which are scattered by the primary collimator in the presence of dispersion. We do not only investigate elastic kicks but also study the effect of the secondary jaw on particles undergoing momentum changes in the primary jaw.

In principle we have to follow the same way of reasoning as for the one-dimensional collimation system of Section 4. Instead of the geometrical method we derive the value of the critical kick K_c analytically here. Assume a particle at its outermost location on its phase ellipse touching the primary collimator and which has a certain momentum deviation^h $\delta = \delta_{\text{in}}$. Its coordinates are

$$X = n_1, \quad X' = \delta_{\text{in}} \chi'_1. \quad (35)$$

In the jaw it receives a kick K and a change of fractional momentum from δ_{in} to δ_{out} . The betatron coordinates of the particle when leaving the jaw are then

$$X_\beta = X - \delta_{\text{out}} \chi_1 = n_1 - \delta_{\text{out}} \chi_1 \quad \text{and} \quad X'_\beta = \delta_{\text{in}} \chi'_1 + K - \delta_{\text{out}} \chi_1 \quad (36)$$

At a secondary collimator located at a phase advance μ downstream of the primary jaw the excursion of the particle is

$$X_{\text{sec}} = X_\beta \cos \mu + X'_\beta \sin \mu + \delta_{\text{out}} \chi_2 \quad (37)$$

where χ_2 is the normalised dispersion at the location of the secondary jaw. Again we would like to know the critical kick K_c pushing the particle exactly on the aperture n_2 of the secondary jaw, i.e. $X_{\text{sec}} = n_2$ (Trenkler¹⁹). Using (36) in (37) we get

^hOf course this implies that either δ is fixed or at least is a slowly changing parameter.

$$K_c = \frac{n_2 - n_1 \cos \mu}{\sin \mu} + \delta_{\text{out}} \frac{\chi_1 \cos \mu - \chi_2}{\sin \mu} + (\delta_{\text{out}} - \delta_{\text{in}}) \chi_1'. \quad (38)$$

For no momentum deviation ($\delta_{\text{in}} = \delta_{\text{out}} = 0$) (38) reduces to formula (3) of Section 4, while the last term vanishes if the particle loses no momentum in the primary jaw ($\delta_{\text{in}} = \delta_{\text{out}}$).

9.2.1 The special case of a straight section ($\rho = 0$) We consider the important special case of a straight section without bending magnets or only with weak bending magnets compared to the main dipoles of the ring. In this case the dispersion behaves like a betatron wave and propagates thus with the transfer matrix:

$$\chi_2 = \chi_1 \cos \mu + \chi_1' \sin \mu. \quad (39)$$

Inserting this into (38) we get

$$K_c = \frac{n_2 - n_1 \cos \mu}{\sin \mu} - \delta_{\text{in}} \chi_1'. \quad (40)$$

We observe three important consequences:

1. The critical kick is independent of the momentum change $\Delta\delta = \delta_{\text{out}} - \delta_{\text{in}}$ in the jaw (δ_{out} does not appear in the formula). This implies that moderate momentum changes (for example due to single diffractive interactions) in the jaw for which chromatic effects do not dominate the kinetic behavior have no influence on the efficiency of the collimation system.
2. If we want to make K_c small in a wide range of positive and negative δ we have to make it independent of δ , i.e. we have to demand

$$\chi_1' = 0 \quad \text{or in non-normalised coordinates} \quad D_1' = -\frac{\alpha_1}{\beta_1} D_1. \quad (41)$$

For elastic scattering this important condition has for the first time been derived and interpreted by Bryant and Klein.¹⁵ Here we put it into a wider context by discovering its validity even in the case of inelastic scattering in the jaw. If $\chi_1' = 0$, K_c gets independent of δ which means that the quality of the collimation system is the same for all energy deviations. This property is obtained by fixing a quantity at the primary jaw (namely χ_1') and is not dependent on any parameter concerning the secondary jaws. Thus the location of the secondary collimators can be chosen independently of momentum collimation considerations. For instance one can place them in the most convenient way for betatron collimation as discussed in the previous sections.

3. The independence of K_c on $\Delta\delta$ has also a negative consequence. A particle which receives a kick $K < K_c$ passes the secondary collimator even if it has a large δ_{out} . The particle will be lost soon behind the straight collimation section, where dispersion starts to differ from its betatron behavior due to bending magnets. This effect cannot be avoided in a straight section and its impact on the machine must be investigated in each individual case.

4. For completeness we state another result of Bryant and Klein.¹⁵ The slope of the primary-beam envelope at the primary collimator is in general δ dependent:

$$X'_{\text{env}} = \delta \chi'_1 \quad (42)$$

in normalised coordinates. Hence if (41) holds it gets independent of momentum deviations. Thus the quality of the longitudinal alignment of the primary collimator gets independent of δ when the collimation condition (41) holds.

One can show that the collimation condition (41) leaves the K -plots of the two-dimensional betatron collimation systems discussed in Sections 5, 6 and 7 unchanged. As kicks and coordinates add quadratically to amplitudes the envelope of the beam in amplitude space gets of course dependent on the local dispersion. All these considerations which are not derived here for brevity show that condition (41) remains valid.

9.2.2 The general case ($\rho \neq 0$) continued We return now to the general case of an arbitrary optics allowing the presence of bending magnets. In general normalised dispersion is determined by the equation

$$\frac{d^2 \chi}{d\mu^2} + \chi = \frac{\beta \sigma}{\rho} \quad (43)$$

where ρ is the local bending radius. This equation is solved by

$$\chi = \chi_1 \cos \mu + \chi'_1 \sin \mu + \int_0^s \frac{\sigma(t)}{\rho(t)} \sin(\mu - \mu(t)) dt, \quad (44)$$

with $s = 0$ being the location of the primary jaw, $\mu(s)$ the phase advance with respect to this point, $\sigma(s)$ the transverse r.m.s. beam radius and s being the running longitudinal coordinate (i.e. the position of the secondary jaw). Expressing χ_2 in (38) by this formula we get the result

$$K_c = \frac{n_1 - n_2 \cos \mu}{\sin \mu} - \delta_{\text{in}} \chi'_1 + \delta_{\text{out}} [a_1(s) \cot \mu - a_2(s)] \quad (45)$$

with

$$a_1(s) = \int_0^s \frac{\sigma(t)}{\rho(t)} \sin \mu(t) dt \quad \text{and} \quad a_2(s) = \int_0^s \frac{\sigma(t)}{\rho(t)} \cos \mu(t) dt. \quad (46)$$

The coefficients a_1 and a_2 are s -dependent. Thus it seems difficult to make (45) independent of the momentum deviations at all collimator positions. Fortunately a_1 and a_2 stay irrelevantly small if only weak bending magnets are involved in the collimation section.

This is the case in the collimation system studied for LHC so far, which contains weak dog-leg bending magnets²⁰ to remove inelastic secondary particles. In this case (41) can be used as a very good approximation. Of course other scenarios using strong bending magnets could be investigated for other machines. In this case one has to use formula (45) and try the best in making it momentum independent.

10 CONCLUSIONS

We studied two-stage collimation systems in terms of extent of the secondary beam halo. While the ultimate theoretical limit is reached in a one-dimensional system with two secondary jaws correctly placed, this limit cannot be reached in a two-dimensional system with a reasonable number of collimators. Nevertheless a good result can be reached with three circular (in normalised coordinates) collimators correctly placed in various optics. We also propose analytical rules for building a two-stage momentum collimation system, which can be combined or not to a betatron system.

REFERENCES

1. L. Burnod, J.B. Jeanneret, Beam Losses and Collimation in the LHC: A Quantitative Approach, CERN SL/91-39 (EA), LHC Note 167 (1991).
2. J.B. Jeanneret, Momentum Losses and Momentum Collimation in LHC, A First Approach, CERN SL/92-44 (EA), LHC Note 211 (1992).
3. J.B. Jeanneret, Momentum Losses in LHC: The Special Case of RF Uncaptured Protons, CERN SL/Note 92-56 (EA) (1992).
4. A. Van Ginneken, Elastic Scattering in Thick Targets and Edge Scattering, Phys. Rev. **D37**, 3292 (1988).
5. J.B. Jeanneret, T. Trenkler, Collimation in LHC: The Scattering Processes, CERN SL Report to be issued.
6. J.B. Jeanneret and T. Trenkler, The Secondary Off-Momentum Particle Tracking Program (SOFT), CERN SL/Note (AP), to be issued.
7. L. Burnod, G. Ferioli, J.B. Jeanneret, Drift Speed measurements of the halo in the SPS Collider, CERN/SL/90-01 (EA), LHC Note 117 (1990).
8. T. Risselada, The effect of the betatron tune on the impact parameter at LHC primary Collimators, CERN/SL/Note 92-16 (AP) (1992).
9. M. Seidel, The Proton Collimation System of HERA, DESY 94-103 (1994).
10. T. Trenkler, J.B. Jeanneret, K2: A Software Package Evaluating Collimation Systems in Circular Colliders (Manual), CERN SL/Note 94-105 (AP) (1994).
11. The LHC Study Group, LHC — The Large Hadron Collider Accelerator Project, CERN/AC/93-03(LHC), (1993).
12. L.C. Teng, Design concepts for the beam scraper system of the main ring, Int. Report Fermilab, FN-196/0400, (1969).
13. J.B. Jeanneret, Phase Difference between Collimators in a Collider, SL/EA/Note 90-01 (1990).
14. M.A. Maslov, N.V. Mokhov, I.A. Yazynin, The SSC Beam Scraper System, SSCL-484 June 1991.
15. P.J. Bryant, E. Klein, The Design of Betatron and Momentum Collimation Systems, CERN SL/92-40 (AP) (1992).
16. J.B. Jeanneret, An Elementary Approach of a Two-Dimensional Collimation System for LHC, CERN SL/Note 92-65 (EA) (1992).

17. T. Trenkler, The Optimum Set of Circular Collimators for Global Two Stage Betatron Collimation Compared to Realistic Systems, CERN SL/93-10(EA), LHC Note 217 (1993).
18. T. Trenkler, L. Burnod, J.B. Jeanneret, The Optics and Layout of the Cleaning Insertion of LHC for a Betatron-Momentum Collimation System, CERN SL/Note 93-45(EA) (1993).
19. T. Trenkler, The Optimum Phase Advance in a Two-Stage Collimator System, CERN SL/92-50 (EA) (1992).
20. J.B. Jeanneret, T. Trenkler, LHC Cleaning Insertion: Some Parameters for the Dog-Leg and the Warm Quadrupoles, SL/Note 94-94 (AP), LHC Note 304 (1994).